



# Modeling and analysis of force prediction in milling process of unidirectional fiber reinforced polymer composites

Haijin Wang<sup>1</sup> · Huiyue Dong<sup>1</sup> · Yinglin Ke<sup>1</sup> · Jie Sun<sup>2</sup>

Received: 26 March 2018 / Accepted: 18 November 2018 / Published online: 15 December 2018  
© Springer-Verlag London Ltd., part of Springer Nature 2018

## Abstract

The cutting force is one of the main factors that influence the processing quality of fiber-reinforced polymer composites (FRPs). However, since the material removal mechanics of composites are quite different from those of metals, the cutting mechanisms of metals cannot be directly used for orthogonal cutting of composites. This paper aims to develop a novel force prediction model without the need to run any experiments. The deformation of fiber and the support of surrounding matrix are analyzed based on the minimum potential energy principle and the dynamic equilibrium. A force prediction model of FRP cutting is obtained for fiber orientations ranging from 0 to  $90^\circ + \gamma$ . The relevant experiments conducted showed the validity of the proposed model. The influence of rake angle and clearance angle on cutting force is analyzed.

**Keywords** Fiber reinforced polymer composites · Fiber fracture · Debonding · Orthogonal cutting

## 1 Introduction

Fiber-reinforced polymer composites (FRPs) are being used extensively in various areas, such as the aerospace, automobile, sports, and energy industries, owing to their high strength-to-weight ratio, high damping ability, low density, etc. In Boeing 787 airplanes, 50% (by weight) of the primary aircraft structures are made of composite [1].

Owing to near net shape fabrication, FRP application needs fewer machining operations than metal materials. However, drilling and milling are still necessary to give the FRP parts their final shape to satisfy assembly

accuracy. Because of the non-homogeneous, anisotropic and reinforced by fiber, it is difficult to predict cutting forces reliably for FRPs [2, 3]. According to the analytical approaches, the investigations on cutting FRPs can be assessed as follows.

### 1.1 Experimental studies

Many recent experimental studies of FRP machining are on the following issues: FRP properties and fiber orientations [4, 5], tool materials and geometries [6, 7], and processing parameters [8, 9]. Hocheng et al. [10] observed chip formation, surface roughness, and cutting forces from milling FRPs. It was found that surface quality depends on the fiber direction. When fibers were parallel to the cutting direction, this yielded a good surface compared to perpendicular ones. Davim et al. [11, 12] reported that the feed rate was the main parameter that affected the machining force in milling of composite materials. Madhavan et al. [13] observed that the variation of cutting force with fiber orientation angle was dependent on the feed. For large feeds, the cutting force increased with the fiber orientation angle until an angle of  $90^\circ$  was reached, whereas for low feeds, the cutting force decreased beyond  $65^\circ$ . Zenia et al. [14] investigated the interaction between machining parameters and the cutting forces, induced cutting damage of CFRP composites. It was found that the increase in the fiber

✉ Huiyue Dong  
donghuiyue@zju.edu.cn

Haijin Wang  
wo1004@163.com

Yinglin Ke  
ylke@zju.edu.cn

Jie Sun  
sunjie@sdu.edu.cn

<sup>1</sup> The State Key Lab of Fluid Power Transmission and Control, School of Mechanical Engineering, Zhejiang University, Hangzhou 310027, China

<sup>2</sup> School of Mechanical Engineering, Shandong University, Ji'nan 250061, China

orientation and the depth of cut lead to the increase in cutting force and induced damage levels.

## 1.2 Numerical simulation

Since the past two decades, a lot of researches have been done on numerical solutions for cutting composite materials, and all of them can be generally divided into two categories: macro-mechanical approaches and micro-mechanical approaches [15]. Xu et al. [16] used cohesive zone concept to simulate the chip formation by FEM. Under the condition that fiber orientation was less than  $\pi/2$ , Rao et al. [17, 18] predicted the damage and chip formation mechanism in ABAQUS. They modeled the composite material as a multiphase material with cohesive zones as the interface between fibers and matrix material. Chakladar et al. [19] established an equivalent elastic macro-mechanical model for the woven composite workpiece and estimated the drilling responses using finite element. Calzada et al. [20] used continuum elements to develop an interfacial model that allowed failure to take place in either tension or compression. The model was able to describe the fiber failure mode occurred in the chip formation process.

## 1.3 Theoretical models

Only few investigations have tended to focus on the theoretical model on the cutting of FRP materials. They used mostly the orthogonal cutting configuration of unidirectional FRPs [21]. Based on the minimum energy theory, Takeyama et al. [22] proposed an analytical model to estimate the horizontal and vertical force in orthogonal cutting. Based on the Merchant theory, Bhatnagar et al. [23] presented an approach to predict the sensitivity of cutting forces to fiber orientations, and the calculated forces showed good agreement with the measured values especially for fiber orientations were lower than  $60^\circ$ . Pwu et al. [24] investigated the cutting mechanism for modeling the chip formation under the condition that the cutting orientation perpendicular to fiber orientation and established an analytical model based on the beam theory, linear elastic fracture, and composite mechanics. Zhang et al. [25, 26] developed a mechanical model to predict forces during the orthogonal cutting of unidirectional FRP with different orientations below  $90^\circ$ .

The above literature review shows that the study of FRP cutting is generally limited to three categories. However, the theoretical analysis is significantly lacking. Some simple models are based on conventional metal cutting mechanics that ignored the interface behavior of composites, and other micro-mechanical models usually need to run a few experiments to obtain some parameter used in the models. In this paper, a modified version of their suggested cutting mechanisms is used to establish an approximate

mechanics model in FRP cutting. The objective of this study is to develop a theoretical approach to obtain cutting forces without the need to run any experiments. Relevant experiments are carried out to examine the model established, and the predicted values are consistent with the experimental results.

## 2 Orthogonal cutting model

### 2.1 The principle

Zhang et al. [25] suggested that the deformation of fiber was different when the fiber orientation limited into the range of  $0$  to  $90^\circ$  and the range of  $90$  to  $180^\circ$  (Table 1 shows the list of symbols used). Taking into account of the tool rake angle, the mechanics models of cutting were different when  $\theta \leq 90^\circ + \gamma$  or when  $\theta > 90^\circ + \gamma$ . This study will focus on the case of  $0 \leq \theta \leq 90^\circ + \gamma$ , as shown in Fig. 1. The modeling for  $\theta > 90^\circ + \gamma$  will be discussed in a separate paper.

In this model, it is assumed that the fibers are bent firstly. Then, they are cut off and slipped on the rake face of tool due to the movement of cutting tool. Consider a single fiber, as shown in Fig. 1, the cutting forces of FRPs can be divided into three major areas: portions A, B, and C. For region A, fraction occurs at the cross-section of fibers. In region B, the workpiece is compressed by the flank face of tool and bounced back when the cutting edge moves forward. The debonding between the matrix and the fiber exists in region C.

In order to develop the mechanics model for cutting processes, some assumptions for analysis are proposed as follows [26, 27].

- (1) The width of the workpiece is equal to the diameter of the fiber.
- (2) Normal stress in the fiber that produces no mechanical work during deformation of the fiber.
- (3) Fiber fracture is taken place when the maximum tensile stress exceeds its tensile strength.
- (4) There is no matrix extension or compression happened.
- (5) In Fig. 1, the part of fiber that above the tool–fiber contact point is compressed by the chip on the rake face and the stress is difficult to calculate. For convenience, we assume that the deflection of this part is the same as that of the tool–fiber contact point, and the stress is part of external force “ $F_U$ ”.

As shown in Fig. 2, the positive  $x$ - and  $z$ -directions are defined for convenience, and the part of the FRPs that supports the fiber can be treated as the equivalent homogeneous material (EHM).

**Table 1** Nomenclature

$A_m$	Matrix cross-sectional area surrounded one fiber	$a_p$	Depth of cut
$E_f$	Young’s modulus of the fiber	$\gamma_0$	Rake angle of tool
$E_m$	Young’s modulus of the matrix	$\theta$	Fiber orientation
$L$	Damage length	$\omega$	Deflection of fiber
$L'$	Deformation length of fiber	$k_m$	The modulus of the foundation EHM
$S_m$	Matrix shear strength	$h$	The remove height of cutting edge
$r$	Radius of fiber-matrix representative volume element	$\sigma_b$	Ultimate strength of the fiber
$l$	Width of cutting edge	$r_f$	Fiber radius
$G_m$	Shear modulus of the matrix	$vol_f$	Fiber volume fraction
$I_f$	Second moment of area of the cross section of the fiber	$r_c$	Cutting edge radius
$Q$	Shear force	$\mu$	Friction coefficient
$M$	Bending moment	$\alpha$	Tool clearance angle
$\nu_m$	Poisson ratio of matrix	$\beta$	Friction angle of rake face

From Fig. 2, we can get

$$L' = L + h/\sin\theta \tag{1}$$

In orthogonal cutting,  $h$  is the depth of cut. While in milling and drilling,  $h$  is the cutting depth of cutting edge when the angle between the cutting direction and the fiber is  $\theta$ .

**2.2 Fiber deformation**

The energy balance for a single fiber surrounded by matrix material is divided into four portions: the work done by the external force “ $F_U$ ,” strain energy in the fiber due to bending, shear strain energy of the matrix, the work done by the force that supports the fiber in EHM.

In Fig. 2, the work done by  $F_U$  can be described as

$$W_{Fu} = F_u w|_{s=L} \tag{2}$$

According to the mechanics of materials [28], the deflection of fiber satisfied the condition of slender beam, and the strain energy in the fiber should be expressed as

$$U_f = \frac{1}{2} \int_0^{L'} E_f I_f \left( \frac{d^2 w}{ds^2} \right)^2 ds \tag{3}$$

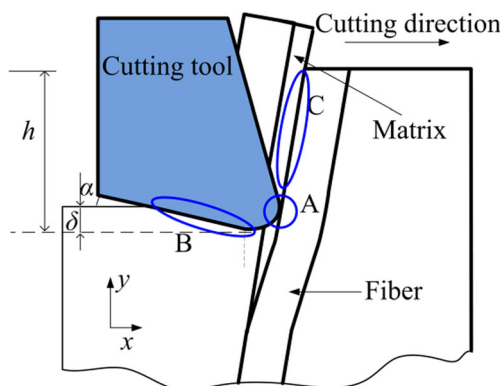


**Fig. 1** Cutting force in FRP cutting

The shear strain energy of matrix will be

$$U_m = \frac{1}{2} \int_0^{L'} \frac{A_m \tau_m^2}{G_m} = \frac{1}{2} A_m G_m \left( \frac{r}{r_f} \right)^2 \int_0^{L'} \left( \frac{dw}{ds} \right)^2 ds \tag{4}$$

where

$$A_m = \frac{\pi r_f^2 (1 - vol_f)}{vol_f} \tag{5}$$

The work done by the force that supports the fiber can be obtained [26, 29]

$$W_{pb} = \int_0^{L'} p_b w ds = \int_0^{L'} k_m w^2 ds \tag{6}$$

where

$$k_m = \frac{0.95 E_m}{1 - \nu_m^2} \left[ \frac{D^4 E_m}{E_f I_f (1 - \nu_m^2)} \right]^{0.108} \tag{7}$$

and

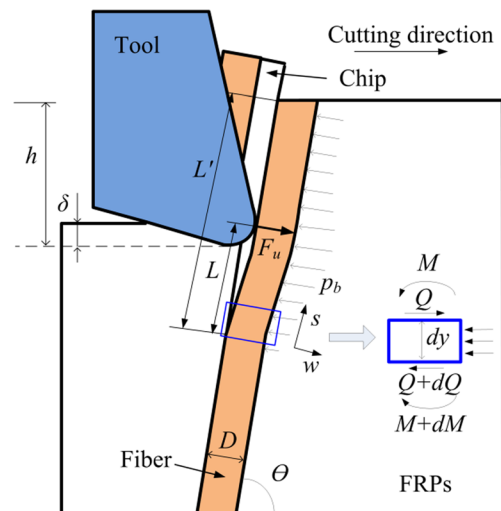


**Fig. 2** Deformation of fiber in cutting

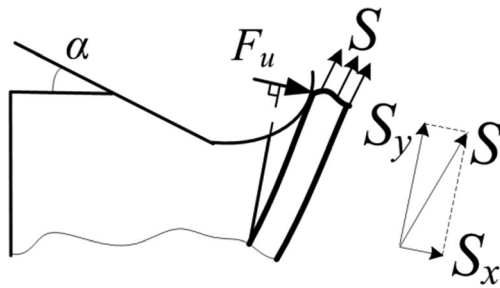


Fig. 3 Fiber fracture in cutting

$$I_f = \pi D^4 / 64 \tag{8}$$

Combining with Eqs. (2), (3), (4), and (6), the energy balance for a single fiber can be shown mathematically as

$$F_u w|_{s=L} - \frac{1}{2} \int_0^L E_f I_f \left( \frac{d^2 w}{ds^2} \right)^2 ds - \frac{1}{2} A_m G_m \left( \frac{r}{r_f} \right)^2 \int_0^L \left( \frac{dw}{ds} \right)^2 ds - \int_0^L k_m w^2 ds = 0 \tag{9}$$

Based on the assumption, fiber fracture is taken place when the maximum tensile stress exceeds its tensile strength. Since the fiber belongs to the brittle material, it is assumed that the load is uniformly distributed in the cross-section for a simplified calculation. As shown in Fig. 3,

$$F_U = \int_0^L p_b ds + S_x = \int_0^L k_m w ds + \sigma_b \pi r_f^2 \frac{w|_{s=L}}{\sqrt{w|_{s=L}^2 + L^2}} \tag{10}$$

If the deflection of fiber  $w$  in Eqs. (8) and (9) is known, the external force “ $F_U$ ” and the damage length “ $L$ ” can be calculated by solving these equations. Therefore, the expression of  $w$  must be obtained from the beam bending theory.

According the beam bending theory [28],

$$\frac{d^2 w}{ds^2} = \frac{M}{E_f I_f} \tag{11}$$

As shown in Fig. 2, when  $y \leq L$ , consider an infinitesimal part of length  $dz$  of the fiber. The equilibrium equation of force and moment should be

$$\begin{cases} Q - (Q + dQ) - p_b ds = 0 \\ M - (M + dM) - (Q + dQ) ds - \frac{p_b ds^2}{2} = 0 \end{cases} \tag{12}$$

Combining Eqs. (10) and (11), we get

$$E_f I_f \frac{d^4 w}{ds^4} - k_m w = 0 \tag{13}$$

According to the assumption (5) and the calculation of Eq. (12), the general solution of  $w$  is

$$w = C_1 e^{\lambda s} + C_2 e^{-\lambda s} + C_3 \cos(\lambda s) + C_4 \sin(\lambda s) \tag{14}$$

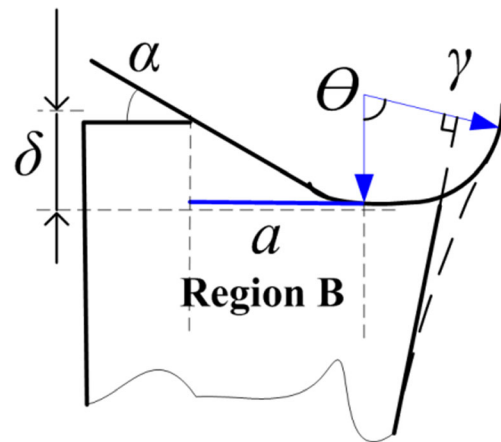


Fig. 4 Contact force between the flank face and the workpiece

where

$$\lambda = \sqrt[4]{\frac{k_m}{E_f I_f}}$$

and  $C_1, C_2, C_3,$  and  $C_4$  are the correlation coefficients.

When the stress caused by the deformation of fiber is increased up to the ultimate strength  $\sigma_b$ , the fracture of fiber will be occurred. And we can get [30]

$$E_f r_f \omega'' = \sigma_b \tag{15}$$

The deflection of the fiber is continuous, so the boundary conditions for the single fiber are as follows:

At the fiber-matrix debonding point ( $s = 0$ ):

$$\begin{cases} w = 0 \\ w'(s) = 0 \end{cases} \tag{16}$$

At the tool–fiber contact point ( $s = L - h / \sin \theta$ )

$$\begin{cases} w'(s) = 0 \\ E_f r_f \omega''|_{s=L} = \sigma_b \end{cases} \tag{17}$$

Therefore, the correlation coefficients can be obtained by solving Eqs. (14), (16), and (17),

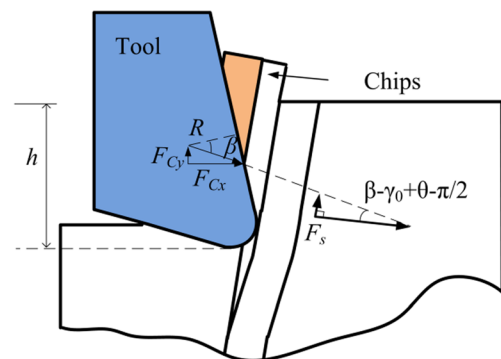
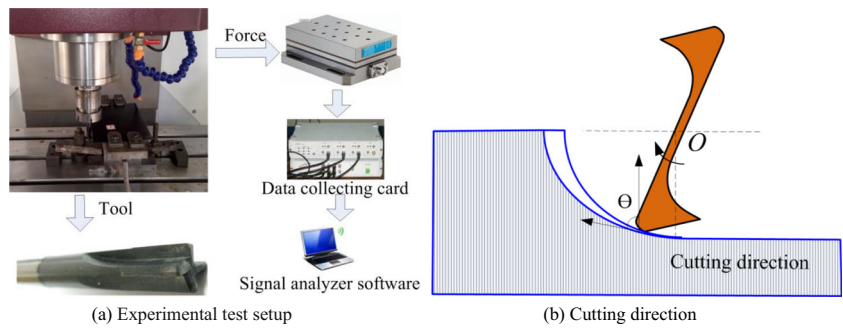


Fig. 5 Fracture of FRPs on the rake face

**Fig. 6** The experiment setup. **a** Experimental test setup. **b** Cutting direction



$$\begin{aligned}
 C_1 &= -\frac{\sigma_b(\sin\lambda L - e^{-\lambda L} + \cos\lambda L)}{2\lambda^2 E_f r_f \sin\lambda L (e^{\lambda L} - e^{-\lambda L})} \\
 C_2 &= \frac{\sigma_b(e^{\lambda L} + \sin\lambda L - \cos\lambda L)}{2\lambda^2 E_f r_f \sin\lambda L (e^{\lambda L} - e^{-\lambda L})} \\
 C_3 &= -\frac{\sigma_b(e^{\lambda L} + e^{-\lambda L} - 2\cos\lambda L)}{2\lambda^2 E_f r_f \sin\lambda L (e^{\lambda L} - e^{-\lambda L})} \\
 C_4 &= \frac{\sigma_b(e^{\lambda L} - e^{-\lambda L} + 2\sin\lambda L)}{2\lambda^2 E_f r_f \sin\lambda L (e^{\lambda L} - e^{-\lambda L})}
 \end{aligned}$$

The deflection of fiber  $w$  will be obtained with the expressions of  $C_1$ ,  $C_2$ ,  $C_3$ , and  $C_4$ . Substituting the value of  $w$  into Eqs. (9) and (10), the cutting force  $F_U$  is determined.

Therefore, the total cutting forces in region A will be

$$\begin{cases} F_{Ax} = F_U \sin\theta + \mu F_U \cos\theta \\ F_{Ay} = -F_U \cos\theta + \mu F_U \sin\theta \end{cases} \quad (18)$$

### 2.3 Deformation of FRPs below the cutting edge

As shown in Fig. 4, the contact force between the flank face and the workpiece material is caused by the bouncing back of the workpiece material. The horizontal force and the vertical force are [25]

$$\begin{cases} F_{Bx} = \frac{1}{2} \mu r_e E_B l \cos^2 \alpha \\ F_{By} = \frac{1}{2} r_e E_B l (1 - \mu \cos \alpha \sin \alpha) \end{cases} \quad (19)$$

**Table 2** Parameters and ranges used for milling experiments

Cutting condition	Cutting tool		
Method	Up milling	Cutting edge radius ( $r_e$ )	5 $\mu$ m
Cutting speed ( $v$ )	94.2 m/min	Rake angle ( $r$ )	7°
Feed rate ( $f_z$ )	0.075 mm/z	Clearance angle ( $\alpha$ )	10°
Depth of cut ( $a_p$ )	3 mm	Diameter	10 mm
Radial depth of cut ( $a_e$ )	5 mm	Number of teeth	4

### 2.4 Fracture of FRPs on the rake face

According to the assumption, the part of fiber that above the tool–fiber contact point is compressed by the chip on the rake face and the stress is calculated as part of “ $F_U$ ” in Section 2.2. When the fractured fiber-matrix representative volume element (RVE) is slipped along the uncut composite materials, the chips are formed in Fig. 5. In region C, the force associated with the matrix shear failure should be evaluated by

$$F_s = \frac{2rhS_m}{\sin\theta} \quad (20)$$

$$R = F_s / \cos(\beta - \gamma_0 + \theta) \quad (21)$$

The horizontal force and the vertical force would be

$$\begin{cases} F_{Cx} = \frac{2rhS_m \sin(\beta - \gamma_0)}{\sin\theta \cos(\beta - \gamma_0 + \theta)} \\ F_{Cy} = \frac{2rhS_m \cos(\beta - \gamma_0)}{\sin\theta \cos(\beta - \gamma_0 + \theta)} \end{cases} \quad (22)$$

### 2.5 The total cutting forces

The total cutting forces,  $F_x$  and  $F_y$ , could be expressed as the summation of the corresponding components for the above three regions,

$$\begin{cases} F_x = F_{Ax} + F_{Bx} + F_{Cx} \\ F_y = F_{Ay} + F_{By} + F_{Cy} \end{cases} \quad (23)$$

where  $F_{Ax}$ ,  $F_{Ay}$ ,  $F_{Bx}$ ,  $F_{By}$ ,  $F_{Cx}$ , and  $F_{Cy}$  are defined in Eqs. (18), (19), and (22).

## 3 Experimental setup

In order to verify the mechanics model, experiments were conducted to measure the cutting forces. The DAEWOO ACE-V500 vertical machining center was used in the

**Table 3** Material properties used in milling experiments

Fiber radius ( $r_f$ )	3.4 $\mu\text{m}$	Poisson's ratio of matrix ( $\nu_m$ )	0.318
Fiber volume fraction ( $vol_f$ )	0.67	Shear modulus of matrix ( $G_m$ )	1.37 GPa
Fiber Young's modulus ( $E_f$ )	260 GPa	Shear strength of matrix ( $S_m$ )	146 MPa
Fiber ultimate strength ( $E_B$ )	5 GPa	Young's modulus of matrix ( $E_m$ )	5.6 GPa
Young's modulus of the bounding area ( $E_B$ )	3.5 GPa		

experiment. The cutting force was measured by Kistler 9129A dynamometer. The experimental setup was shown in Fig. 6. A customized carbide tool with straight flutes as shown in Fig. 6 was designed to conduct the experiments. The depth of cut ( $a_p$ ) is 3 mm, while the radius of milling tool is 5 mm. And it ensures that only a single mill edge is involved in the cutting process at any moment. As shown in Fig. 6b, since the cutting direction was constantly changed in FRP milling, the cutting force could be obtained under different conditions of  $\theta$ . The parameters used and their ranges are presented in Table 2. The CFRP specimen used in the experiment is T700/6421. The composite is a 30-ply (fiber orientation  $90^\circ$ ) laminate, and the thickness of workpiece material was 3 mm. The material properties are given in Table 3.

In order to obtain the cutting thickness when the cutting edge is in an arbitrary position, the milling operation should be converted to orthogonal cutting. As shown in Fig. 7, the cutting length  $l$  and the maximum thickness of undeformed chip can be obtained [31]

$$l = R \cdot \arccos\left(1 - \frac{a_e}{R}\right) \quad (24)$$

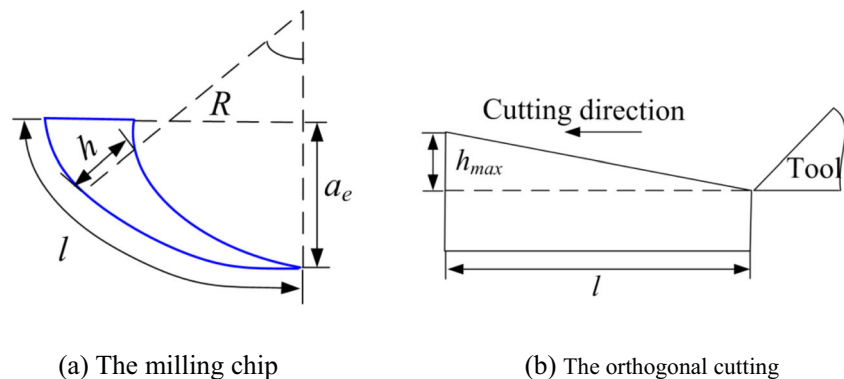
$$h_{\max} = \frac{f_z \sqrt{2Ra_e - a_e^2}}{R} \quad (25)$$

Therefore, the cutting thickness in this experiment can be obtained by solving Eqs. (24) and (25),

$$h = \frac{h_{\max}}{l} f_z \Delta t = \frac{2f_z(\pi/2 - \theta)h_{\max}}{\pi l} \quad (26)$$

**Fig. 7** The conversion of milling.

**a** The milling chip. **b** The orthogonal cutting



## 4 Comparison between analytical and experimental results

Figure 8 shows the difference between the predicted and the actual machining forces. The variation trend of theoretical values is consistent with that of the experimental values, while there is a variance between the predicted and experimental results. This is due to the material properties. The predicted forces are based on the macro-mechanical properties of fiber and matrix. However, the experiment values are influenced by the processing conditions and the FRP properties in small deformation zone.

During a single cutting of the cutting edge, several small peaks are existed for the experimental  $F_x$ . As shown in Fig. 9a, the bending deformation of fibers is generated by the extrusion of cutting edge. Due to the bonding effect between the fiber and the resin, an overall deformation is produced for several fibers. Figure 9b shows the morphology of machined surface, and some broken fibers are bonded together with the resin. Accordingly, the fiber fracture process in FRP milling is shown in Fig. 9c, and adjacent fibers are combined together to form the chip in FRP milling. In the first stage, with the increase of fiber deformation, the cutting force reaches a peak value. In the second stage, the fiber fracture is occurred, and the chips are departed from the workpiece. The cutting edge is not cutting into the composite materials in a short time, and the cutting force decreases at the same time. In the third stage, the cutting tool continues to contact with the workpiece, and the cutting force increases to another peak value.

Accordingly, the theoretical model is effective and can be used in orthogonal cutting of FRPs. Figure 10 shows the force prediction with different rake angles. With the increase of rake

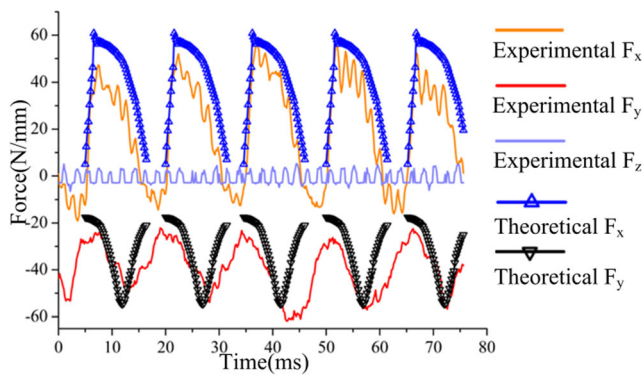


Fig. 8 Comparison between analytical and experimental results

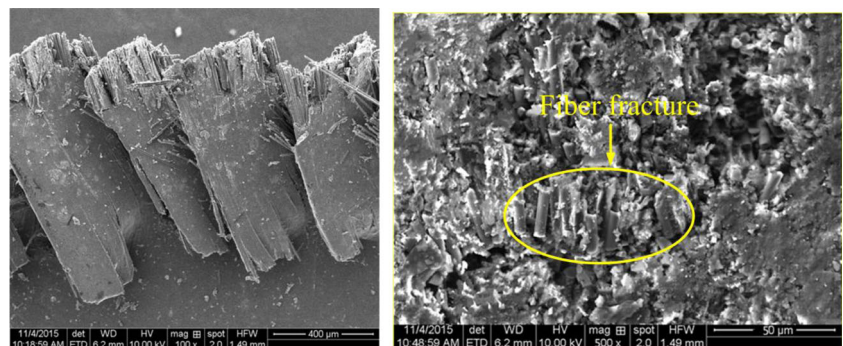
angle, the cutting force is decreased. When the rake angle is large, the deformation of cutting area is small and the cutting edge is sharp, so the composite material is cut off easily by the cutting tool.

Based on Eq. (19), we get

$$\begin{cases} \frac{\partial F_{Bx}}{\partial \alpha} = -\frac{1}{2} \mu r_c E_B l \sin 2\alpha \\ \frac{\partial F_{By}}{\partial \alpha} = -\frac{1}{2} r_c E_B l \mu \cos 2\alpha \end{cases} \quad (27)$$

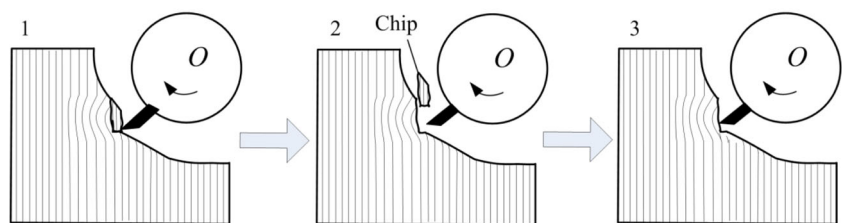
From Eq. (27), it is found that the increase of clearance angle decreases the cutting force of region C. In region C, with the increase of clearance angle, the contact length is smaller and smaller, and so the bouncing back force of machined surface and the friction of tool flank are reduced. However, in the calculation of theoretical model, it is found that the force in the flank face of tool (region B) is one magnitude less than

Fig. 9 The milling of FRPs. a The side face. b The machined surface. c The chip formation



(a) The side face

(b) The machined surface



(c) The chip formation

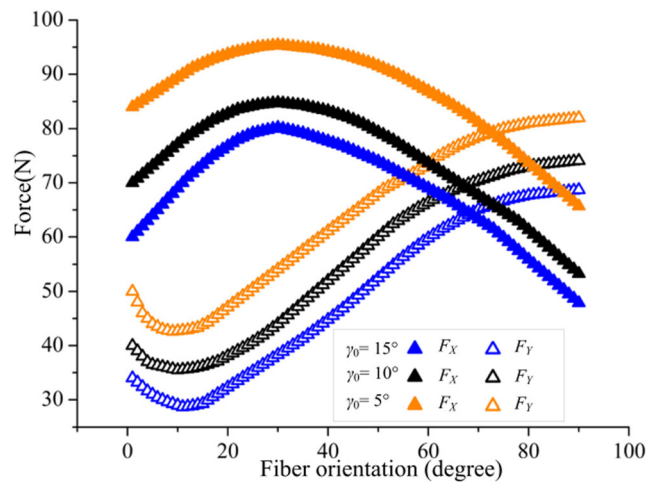


Fig. 10 The force prediction with the changes of rake angle

the force in other areas (regions A and C), so the force in the flank face of tool shares a small proportion of the total cutting force, and the influence of clearance angle on the total cutting force is not obvious.

### 5 Conclusion

In this study, the theoretical model of cutting forces is established in orthogonal cutting of FRPs when  $0 \leq \theta \leq 90^\circ + \gamma$ . Three deformation regions are taken into consideration to develop this model, such as the fiber deformation region, the bouncing back region, and the slipping region.

The influence of rake angle and clearance angle on cutting force is analyzed. The following conclusions can be drawn from the present research endeavor:

- (1) The theoretical model of cutting forces can be used in the prediction of cutting forces without the need to run any experiments in orthogonal cutting of FRPs. The predicted values are consistent with the experimental results.
- (2) In the theoretical prediction of FRP cutting, it was found that the fiber orientation has a significant influence on the changes of cutting force.
- (3) With the increase of rake angle, the cutting force is decreased. However, the influence of clearance angle on the total cutting force is not obvious.

**Funding information** The work was supported by the Major Research plan of the National Natural Science Foundation of China (Grant No. 91748204), the China Postdoctoral Science Foundation (2017M621917), and the Shandong Provincial Natural Science Foundation, China (ZR2017BEE027).

**Publisher's Note** Springer Nature remains neutral with regard to jurisdictional claims in published maps and institutional affiliations.

## References

1. Gilpin A (2009) Tool solutions for machining composites. *Reinf Plast* 53(6):30–33
2. Santiuste C, Olmedo A, Soldani X, Miguelez H (2012) Delamination prediction in orthogonal machining of carbon long fiber-reinforced polymer composites. *J Reinf Plast Compos* 31: 875–885
3. Cong WL, Pei ZJ, Deines TW, Treadwell C (2011) Rotary ultrasonic machining of CFRP using cold air as coolant: feasible regions. *J Reinf Plast Compos* 30:899–906
4. Wang F, Yin J, Ma J, Jia Z, Yang F, Niu B (2017) Effects of cutting edge radius and fiber cutting angle on the cutting-induced surface damage in machining of unidirectional CFRP composite laminates. *Int J Adv Manuf Technol* 91:3107–3120
5. Amin M, Yuan S, Khan MZ, Wu Q, Zhu G (2017) Development of a generalized cutting force prediction model for carbon fiber reinforced polymers based on rotary ultrasonic face milling. *Int J Adv Manuf Technol* 93:2655–2666
6. Li H, Qin X, He G, Jin Y, Sun D, Price M (2016) Investigation of chip formation and fracture toughness in orthogonal cutting of UD-CFRP. *Int J Adv Manuf Technol* 82:1079–1088
7. Zhou L, Ke Y, Dong H, Chen Z, Gao K (2016) Hole diameter variation and roundness in dry orbital drilling of CFRP/Ti stacks. *Int J Adv Manuf Technol* 87:811–824
8. Campos Rubio J, Abrao AM, Faria PE, Correia AE, Davim JP (2008) Effects of high speed in the drilling of glass fibre reinforced plastic: evaluation of the delamination factor. *Int J Mach Tools Manuf* 48(6):715–720
9. Jain NK, Jain VK, Deb K (2007) Optimization of process parameters of mechanical type advanced machining processes using genetic algorithms. *Int J Mach Tool Manu* 47:900–919
10. Hocheng H, Puw HY, Huang Y (1993) Preliminary study on milling of unidirectional carbon fibre-reinforced plastics. *Compos Manuf* 4(2):103–108
11. Davim JP, Reis P, António CC (2004) A study on milling of glass fiber reinforced plastics manufactured by hand-lay up using statistical analysis (ANOVA). *Compos Struct* 64(3–4):493–500
12. Davim JP, Reis P (2005) Damage and dimensional precision on milling carbon fiber-reinforced plastics using design experiments. *J Mater Process Technol* 160(2):160–167
13. Madhavan V, Lipczynski G, Lane B, Whitenon E (2015) Fiber orientation angle effects in machining of unidirectional CFRP laminated composites. *J Manuf Process* 20:431–442
14. Zenia S, Ayed LB, Nouari M, Delamézière A (2015) Numerical analysis of the interaction between the cutting forces, induced cutting damage, and machining parameters of CFRP composites. *Int J Adv Manuf Technol* 78:465–480
15. Dandekar CR, Shin YC (2012) Modeling of machining of composite materials: a review. *Int J Mach Tool Manu* 57:102–121
16. Xu J, El Mansori M (2015) Cutting modeling using cohesive zone concept of titanium/CFRP composite stacks. *Int J Precis Eng Manuf* 16:2091–2100
17. Rao GVG, Mahajan P, Bhatnagar N (2007) Micro-mechanical modeling of machining of FRP composites – cutting force analysis. *Compos Sci Technol* 67:579–593
18. Rao GVG, Mahajan P, Bhatnagar N (2007) Machining of UD-GFRP composites chip formation mechanism. *Compos Sci Technol* 67:2271–2281
19. hakladar ND, Pal SK, Mandal P (2012) Drilling of woven glass fiber-reinforced plastic—an experimental and finite element study. *Int J Adv Manuf Technol* 58:267–278
20. Calzada KA, Kapoor SG, Devor RE, Samuel J, Srivastava AK (2012) Modeling and interpretation of fiber orientation-based failure mechanisms in machining of carbon fiber-reinforced polymer composites. *J Manuf Process* 14:141–149
21. Soussia AB, Mkaddem A, Mansori ME (2014) Rigorous treatment of dry cutting of FRP – interface consumption concept: a review. *Int J Mech Sci* 83:1–29
22. Everstine GC, Rogers TG (1971) A theory of machining of fiber-reinforced materials. *J Compos Mater* 5:94–106
23. Bhatnagar N, Ramakrishnan N, Naik NK, Komanduri R (1995) On the machining of fiber reinforced plastic (FRP) composite laminates. *Int J Mach Tool Manu* 35:701–716
24. Pwu HY, Hocheng H (1998) Chip formation model of cutting fiber-reinforced plastics perpendicular to fiber axis. *J Manuf Sci Eng* 120: 192–196
25. Zhang LC, Zhang HJ, Wang XM (2001) A force prediction model for cutting unidirectional fibre-reinforced plastics. *Mach Sci Technol* 5:293–305
26. Xu W, Zhang LC (2014) On the mechanics and material removal mechanisms of vibration-assisted cutting of unidirectional fibre-reinforced polymer composites. *Int J Mach Tools Manuf* 80–81: 1–10
27. Jahromi AS, Bahr B (2010) An analytical method for predicting cutting forces in orthogonal machining of unidirectional composites. *Compos Sci Technol* 70:2290–2297
28. Beer F, Johnston E, DeWolf J (2002) *Mechanics of materials*. McGraw-Hill, New York
29. Hamermesh M (1958) *Beams on Elastic Foundation: theory with applications in the fields of civil and mechanical engineering*. University of Michigan Press, Ann Arbor, Michigan, United States
30. Boresi AP, Schmidt RJ, Sidebottom OM (1993) *Advanced mechanics of materials*. Wiley, New York
31. Sun Y (2014) Parametric modeling of milling titanium alloy and prediction of tool wear state. Shandong University